Noncanonical role of *Arabidopsis* COP1/SPA complex in repressing BIN2-mediated PIF3 phosphorylation and degradation in darkness

Jun-Jie Ling[a,1], Jian Li[a,1], Danmeng Zhu[a,2], and Xing Wang Deng[a,2]

[a]State Key Laboratory of Protein and Plant Gene Research, Peking-Tsinghua Center for Life Sciences, School of Advanced Agriculture Sciences and School of Life Sciences, Peking University, Beijing 100871, China

Contributed by Xing Wang Deng, February 20, 2017 (sent for review January 19, 2017; reviewed by Meng Chen and Hsu-Liang Hsieh)

The E3 ligase CONSTITUTIVELY PHOTOMORPHOGENIC 1 (COP1) has been known to mediate key signaling factors for degradation via the ubiquitin/26S proteasome pathway in both plants and animals. Here, we report a noncanonical function of *Arabidopsis* COP1, the central repressor of photomorphogenesis, in the form of a COP1/ SUPPRESSOR of *phyA-105* (SPA) complex. We show that the COP1/SPA complex associates with and stabilizes PHYTOCHROME INTERACTING FACTOR 3 (PIF3) to repress photomorphogenesis in the dark. We identify the GSK3-like kinase BRASSINOSTEROID-INSENSITIVE 2 (BIN2) as a kinase of PIF3, which induces PIF3 degradation via 26S proteasome during skotomorphogenesis. Mutations on two typical BIN2 phosphorylation motifs of PIF3 lead to a strong stabilization of the protein in the dark. We further show that the COP1/SPA complex promotes PIF3 stability by repressing BIN2 activity. Intriguingly, without affecting BIN2 expression, the COP1/SPA complex modulates BIN2 activity through interfering with BIN2–PIF3 interaction, thereby inhibiting BIN2-mediated PIF3 phosphorylation and degradation. Taken together, our results suggest another paradigm for COP1/SPA complex action in the precise control of skotomorphogenesis.

photomorphogenesis | COP1/SPA complex | posttranscriptional regulation

In darkness, *Arabidopsis* seedlings undergo skotomorphogenesis, which is a developmental strategy that postgerminated seedlings use to accelerate their growth in soil and optimize the plant shape before reaching to the light (1). Any premature opening of the cotyledon, reduced apical hook, and hypocotyl elongation would impede the pace of life or be fatal to terrestrial flowering plants. The precise control of skotomorphogenesis has been under intensive investigation.

To date, it has been shown that plants use three different groups of signaling factors to repress photomorphogenesis in darkness: CONSTITUTIVELY PHOTOMOROPHOTENIC/ DEETIOLATED/FUSCA (COP/DET/FUS) group proteins and phytochrome-interacting factors (PIFs), and ethylene-insensitive 3 (EIN3)/EIN3-like 1 (EIL1) proteins (2–4). Genetic analyses have indicated that lesions in each of the three group genes cause a defective skotomorphogenesis with different degrees of *cop* phenotypes, as characterized by shorter hypocotyls, opened cotyledons, and overaccumulated protochlorophyllide (5–7). The COP/DET/FUS group repressors belong to three biochemical entities: the COP1/SPA (SUPPRESSOR of *phyA-105*) complex, the CDD (COP10-DET1-DDB1) complex, and the COP9 signalosome, known to mediate the proteolysis of key photomorphogenesis-promoting factors via ubiquitin/26S proteasome pathway (8–10). The PIFs, a small subset of basic helix–loop–helix transcription factors, control the expression of thousands genes to promote skotomorphogenesis, exampled by PIF1, -3, -4, and -5 (11, 12). EIN3/EIL1 have been recently shown to promote etiolation in darkness and phytochrome B can interact with and promote the degradation of EIN3 in red light (13, 14). Strikingly, several molecular connections have suggested that the three group genes synergistically repress photomorphogenesis in the dark (5, 15).

Among COP/DET/FUS factors, the central photomorphogenic repressor COP1 and SPA proteins constitute stable heterogeneous complexes, and function as an E3 ligase to target several key transcription factors for degradation, such as LONG HYPOCOTYL 5 (HY5), HY5 HOMOLOG (HYH), LONG HYPOCOTYL IN FAR-RED 1 (HFR1), and LONG AFTER FAR-RED LIGHT 1 (LAF1) (16–19). COP1 is well conserved in vertebrates and its function as an E3 ligase has been indicated in the lipid metabolism, tumorigenesis, and the stress response (20).

The stability of PIF proteins is tightly controlled by regulated protein degradation (21–23). The key factors that are required for the phosphorylation and ubiquitination of PIFs attract much attention. Importantly, two types of E3 ligases have been shown to mediate the degradation of PIF1 and PIF3, respectively, upon light illumination (24, 25). Moreover, casein kinase II (CKII) and BRASSINOSTEROID INSENSITIVE 2 (BIN2) have been identified as the kinase of PIF1 and PIF4, respectively, which promotes their degradation in response to light (26, 27). However, reports on how the PIFs are regulated in darkness are rather limited, although previous studies have suggested that the accumulation of PIF3, the founding member of PIF, is dependent on COP1 and SPA proteins, as well as DET1 (12, 28, 29). In this study, we identify BIN2 as a kinase of PIF3 that mediates its destabilization, most likely through two BIN2 phosphorylation sites in the dark. Importantly, COP1/SPA blocks the interaction between BIN2 and PIF3, which, in turn, promotes the stability of PIF3. Our results illuminate an additional mechanism for the

Significance

Initially discovered as a central repressor of the seedling photomorphogenesis in plants, and later characterized in animals, the E3 ligase CONSTITUTIVELY PHOTOMORPHOGENIC 1 (COP1) has been shown to have conserved biochemical activities in eukaryotes. In this study, we show that to coordinately promote skotomorphogenesis, the COP1/ SUPPRESSOR of *phyA-105* (SPA) complex represses the activity of the GSK3-like kinase BRASSINOSTEROID-INSENSITIVE 2 (BIN2) in a nonproteolytic manner to stabilize the key repressor of photomorphogenesis PHYTOCHROME INTERACTING FACTOR 3 (PIF3). The COP1/SPA-BIN2-PIF3 module represents an additional layer of COP1/SPA regulation in *Arabidopsis* and is essential for shaping the plants when grown in the dark.

Author contributions: J.-J.L., J.L., D.Z., and X.W.D. designed research; J.-J.L., J.L., and D.Z. performed research; J.-J.L., J.L., D.Z., and X.W.D. analyzed data; and J.-J.L., J.L., D.Z., and X.W.D. wrote the paper.

Reviewers: M.C., University of California, Riverside; and H.-L.H., National Taiwan University.

The authors declare no conflict of interest.

[1]J.-J.L. and J.L. contributed equally to this work.

[2]To whom correspondence may be addressed. Email: zhudanmeng@pku.edu.cn or deng@pku.edu.cn.

This article contains supporting information online at www.pnas.org/lookup/suppl/doi:10.1073/pnas.1700850114/-/DCSupplemental.

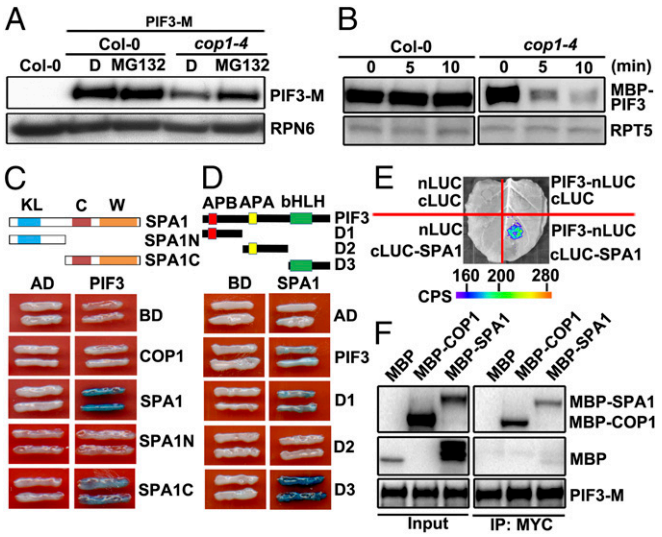

Fig. 1. COP1/SPA complex stabilizes and interacts with PIF3 in the dark. (*A*) Protein levels of PIF3-M in Col-0 and *cop1–4* background with or without MG132 treatment. RPN6 was used as a loading control. D, DMSO. (*B*) Cell-free degradation of MBP-PIF3 protein in the extracts of Col-0 and *cop1–4*. RPT5 was used as a loading control. (*C*) PIF3 interacts with SPA1 in yeast cells. C, coil domain; KL, kinase-like domain; SPA1N (residues 1–545 aa); SPA1C (residues 546–1,029 aa); W, WD40 domain. (*D*) Mapping of SPA1-interacting regions of PIF3 in yeast cells. Full-length and truncated PIF3 were fused with AD. Full-length SPA1 was fused with BD. PIF3-D1 (1–180 aa), D2 (181–338 aa), D3 (339–524 aa). (*E*) LCI assays showing the interaction of SPA1 and PIF3 in *N. benthamiana* leaf cells. cLUC, the vector containing C-terminal fragment of firefly luciferase; nLUC, the vector containing N-terminal fragment of firefly luciferase. Empty vectors were used as negative controls. (*F*) The Co-IP assays showing COP1/SPA1 complex associates with PIF3.

control of key transcription factor stability by the COP1/SPA complex to achieve the accurate regulation of skotomorphogenesis in the model plant *Arabidopsis*.

Results

COP1/SPA Complex Stabilizes PIF3 in the Dark. To study the role of COP1 and SPAs in the regulation of PIF3 stability, we verified PIF3 levels in COP1/SPA complex mutants. In agreement with previous reports, levels of PIF3 were nearly undetectable in the dark-grown *cop1–4*, as well as in the quadruple *spa1 spa2 spa3 spa4* (*spaQ*) mutant (Fig. S1). To investigate the posttranscriptional regulation of PIF3, a 35S:PIF3-HIS-MYC (PIF3-M)/*cop1–4* line was generated and examined. Immunoblot analysis showed that the abundance of PIF3-M in *cop1–4* was notably lower than the WT, and was significantly increased when treated with the proteasome inhibitor MG132 (Fig. 1*A*). This finding indicates a higher than normal degradation of PIF3-M by 26S proteasome in *cop1–4*. Next, the faster degradation of PIF3 in *cop1–4* was recapitulated in a cell-free system. The recombinant MBP (MALTOSE BINDING PROTEIN)-PIF3 was quite stable in the extracts from dark-grown WT seedlings, but was degraded rapidly in the extracts from *cop1–4* seedlings (Fig. 1*B*), supporting a stabilizing role of COP1/SPA complex on PIF3 in the dark.

COP1/SPA1 Complex Interacts with PIF3 via SPA1. To examine whether the COP1/SPA complex interacts with PIF3, we performed yeast two-hybrid analysis. As shown in Fig. 1*C*, the representative SPA protein SPA1, but not COP1, interacted with PIF3 in yeast cells. Moreover, the C terminal of SPA1 spanning the coiled-coil domain and WD40 domain was required for its interaction with PIF3 (Fig. 1*C*). Meanwhile, our results showed that both N- and C-terminal regions of PIF3 were required for its interaction with SPA1 (Fig. 1*D*). To verify the interaction between PIF3 and SPA1 in vivo, we first took advantage of the firefly luciferase complementation-imaging (LCI) assay. Indeed, when PIF3-nLUC and cLUC-SPA1 were coexpressed in tobacco leaves transiently, the activity of luciferase was reconstituted, indicating that SPA1 directly interacts with PIF3 (Fig. 1*E*). We then used a coimmunoprecipitation (Co-IP) assay to test the association of the COP1/SPA1 complex with PIF3. As expected, when PIF3-M was immunoprecipitated with an anti-MYC affinity matrix in the extracts supplemented with the recombinant MBP, MBP-COP1, or MBP-SPA1 proteins, both MBP-COP1 and MBP-SPA1 could be retrieved, respectively, but not MBP (Fig. 1*F*). Next, we examined the possible genetic interaction of COP1/SPA and PIF3. Compared with the fully opened cotyledons of *cop1–4* mutants, overexpression of PIF3-M in *cop1–4* exhibited much less expanded cotyledons (Fig. S2). Taken together, our results suggest that the COP1/SPA complex functionally acts together with PIF3 in darkness.

The Gain-of-Function *bin2-1* Mutation Leads to PIF3 Destabilization in the Dark. The key repressor of brassinosteroid (BR) signaling BIN2 has been shown to be a kinase that phosphorylates PIF4 and mediates its destabilization via the proteasome pathway (27). This result prompted us to examine whether PIF3 is also a phosphorylation target of BIN2. Interestingly, in our protein blot assay we found that the abundance of PIF3 was dramatically decreased in *bin2-1* compared with WT (Fig. 2*A*). The MG132 treatment recovered the PIF3 level in *bin2-1*, suggesting that PIF3 was regulated by BIN2-mediated degradation through the 26S proteasome (Fig. 2*A*). Similarly, in the cell-free degradation system we observed that the recombinant MBP-PIF3 protein in WT extracts displayed a slow rate of degradation, whereas it was rapidly degraded in *bin2-1* (Fig. 2*B*). This finding suggests a requirement of BIN2 activation for PIF3 degradation in the dark.

Mutations on Two BIN2 Recognition Motifs of PIF3 Enhance Its Stability in the Dark. To investigate whether BIN2 physically interacts with PIF3, we performed a yeast two-hybrid assay. As expected, BIN2 had a positive interaction with PIF3 in yeast cells (Fig. 2*C*). Interestingly, the interaction regions of PIF3 with

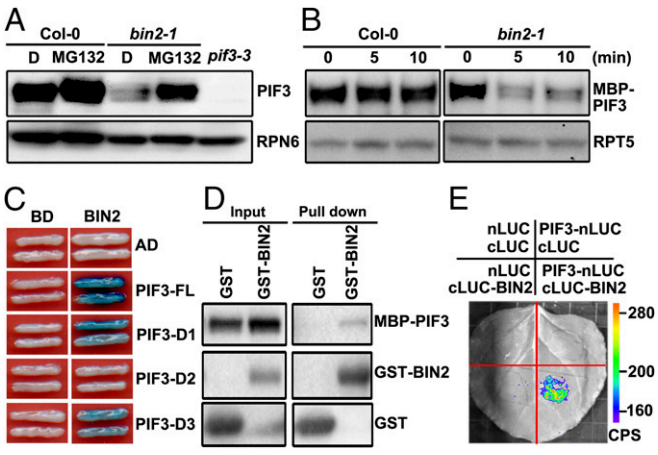

Fig. 2. Constitutive activation of BIN2 mediates the proteasomal degradation of PIF3 in the dark. (*A*) Levels of PIF3 in Col-0 and *bin2-1*. RPN6 was used as a loading control. D, DMSO. (*B*) Cell-free degradation of MBP-PIF3 protein was accelerated in *bin2-1* mutant extracts. RPT5 was used as a loading control. (*C*) BIN2 interacts with PIF3 in yeast cells. Full-length and truncated PIF3 were fused with AD. Full-length BIN2 was fused with BD. (*D*) In vitro pull-down assays showing the direct interaction of MBP-PIF3 with GST-BIN2. MBP-PIF3 was used as the prey molecules and incubated with GST-BIN2 or GST. (*E*) LCI assays showing the interaction of BIN2 with PIF3 in *N. benthamiana* leaf cells.

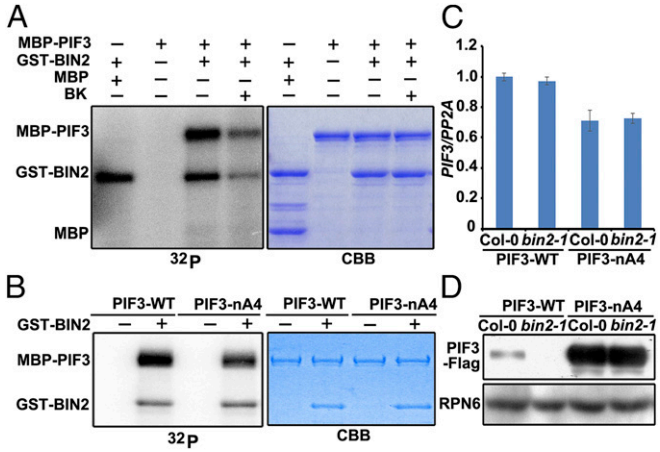

Fig. 3. BIN2 phosphorylates and modulates PIF3 stability in the dark. (*A*) BIN2 phosphorylates PIF3 in vitro. MBP or MBP-PIF3 was incubated with [γ-^{32}P] ATP, without or with GST-BIN2: (*Left*) the autoradiogram, (*Right*) Coomassie brilliant blue (CBB) staining. BK is an *Arabidopsis* GSK3-like kinase inhibitor. (*B*) Phosphorylation of MBP-PIF3 and MBP-PIF3-nA4 by BIN2. Kinase assays were performed with GST-BIN2 and MBP-PIF3 or MBP-PIF3-nA4: (*Left*) the autoradiogram, (*Right*) CBB staining of the gel. (*C*) mRNA levels of *PIF3-WT-Flag* and *PIF3-nA4-Flag* in Col-0 and *bin2-1*. The relative levels were normalized to *PP2A*. (*D*) Protein gel blot of PIF3-WT-Flag and PIF3-nA4-Flag fusion proteins in Col-0 and *bin2-1*. RPN6 was used as a loading control.

BIN2 turned out to be the same domains that mediate PIF3–SPA1 interaction (Fig. 2*C*). Using in vitro pull-down and firefly LCI assays, we further proved the direct interaction of BIN2 with PIF3 in vitro and in vivo (Fig. 2 *D* and *E*). Thus, these data indicate that BIN2 modulates PIF3 degradation through their direct interaction.

Next, we conducted in vitro kinase assays with MBP-PIF3 and GST-BIN2, which clearly suggested a direct phosphorylation of PIF3 by BIN2 (Fig. 3*A*). We therefore searched for the putative serine (S)/threonine (T) recognition site, the short BIN2 consensus motif (S/T)-X-X-X-(S/T) in PIF3. The motif analysis identified 14 putative BIN2-recongnition motifs in the PIF3 protein sequence (Fig. S3). Among them, only two motifs (T^{220}KEKS^{224}, S^{283}SVGS^{287}) were conserved in both dicot and monocot species (Fig. S3). We therefore introduced alanine mutations to replace S/T residues in the two conserved motifs, generating the PIF3-nA4 mutant protein, which led to its reduced phosphorylation in vitro (Fig. 3*B*). Importantly, the abundance of PIF3-nA4-Flag in the transgenic seedlings was found to be significantly higher than that of PIF3-WT-Flag, when *PIF3-WT-Flag* and *PIF3-nA4-Flag* transcript levels are similar (Fig. 3 *C* and *D*). These data indicate that mutation of the two BIN2 phosphorylation sites results in the strong stabilization of PIF3 in the dark. Consistent with this result, when *35S:PIF3-WT-Flag* and *35S:PIF3-nA4-Flag* lines were each crossed to the *bin2-1* mutant, we observed that constitutive activation of BIN2 in these transgenic seedlings caused a strong decrease in PIF3-WT-Flag protein level, but had little effect on PIF3-nA4-Flag protein stability (Fig. 3*D*). These data again demonstrate that these two conserved BIN2 phosphorylation motifs are essential for PIF3 stability regulation in the dark.

COP1/SPA Inhibits BIN2-Mediated PIF3 Destabilization. To further study the opposite effect of COP1/SPA and BIN2 on the regulation of PIF3 stability, PIF3-M/*cop1–4 bin2-3 bil1 bil2* was generated by genetic crossing. When *BIN2* and its two closest homologs *BIN2 like 1* (*BIL1*) and *BIN2 like 2* (*BIL2*) were depleted in *cop1–4* background, the abundance of PIF3-M was recovered to that in WT. This result suggests that *BIN2* and its related genes act downstream of *COP1* to destabilize PIF3 (Fig. 4*A*). Meanwhile, when *35S:PIF3-WT-Flag* and *35S:PIF3-nA4-Flag* lines were each crossed to the *cop1–4* mutant, we observed that PIF3-nA4-Flag was strongly stabilized in *cop1–4* (Fig. 4*B*), supporting that the phosphorylation of PIF3 by BIN2 is downstream of COP1 in the regulation of PIF3 stability. Similarly, overexpression of PIF3-nA4-Flag in *cop1–4* displayed much less expanded cotyledons (Fig. S4).

Next, to check whether COP1/SPA and BIN2 have direct interaction, we performed yeast two-hybrid and in vitro pull-down assays. We detected that COP1, but not SPA1, physically interacted with BIN2 in vitro (Fig. S5 *A* and *B*). Moreover, our Co-IP analysis showed that BIN2–Flag fusion protein expressed from the dark-grown 35S:BIN2-Flag/*Col* seedlings coimmunoprecipitated COP1, further supporting BIN2–COP1 interaction in vivo (Fig. S5*C*). These results led us to examine whether COP1 affects the accumulation of BIN2 in the dark. To this end, *35S:BIN2-Flag* was introduced into WT background, and each of the resulting two independent lines was crossed into *cop1–4* mutant to generate the homozygous plants (Fig. 4*C*). Interestingly, the abundance of BIN2-Flag from both lines in Columbia-0 (Col-0) was comparable to that in *cop1–4*, suggesting that the level of BIN2 is not affected by COP1 (Fig. 4*D*).

COP1/SPA Complex Interferes with BIN2–PIF3 Interaction in the Dark. Given that SPA1 and BIN2 interacts with the same regions of PIF3, COP1 directly interacts with BIN2, and that the COP1/SPA complex and BIN2 have an antagonistic role in regulating PIF3 stability, we speculated that COP1/SPA may interfere with BIN3–PIF3 interaction. Using a modified yeast three-hybrid system, we found that the interaction between PIF3 and BIN2 indicated by the β-galactosidase activity was greatly reduced when COP1 or SPA1, but not the GFP protein, was coexpressed in yeast cells (Fig. 5*A*). This result suggests that the presence of COP1 or SPA1 alone may interfere with the BIN2–PIF3 interaction. To further investigate whether the BIN2–PIF3 interaction could be interfered by COP1/SPA complex in *Arabidopsis*, we performed a Co-IP analysis using extracts from transgenic lines expressing *35S:PIF3-HIS-MYC* in WT and *cop1–4* mutant, each supplemented with the same amount of recombinant GST-BIN2. As expected, although less than threefold of PIF3-M fusion protein was coimmunoprecipitated using anti-MYC conjugated beads in the total extracts of *cop1–4* seedlings than the WT, the yields of GST-BIN2 were similar,

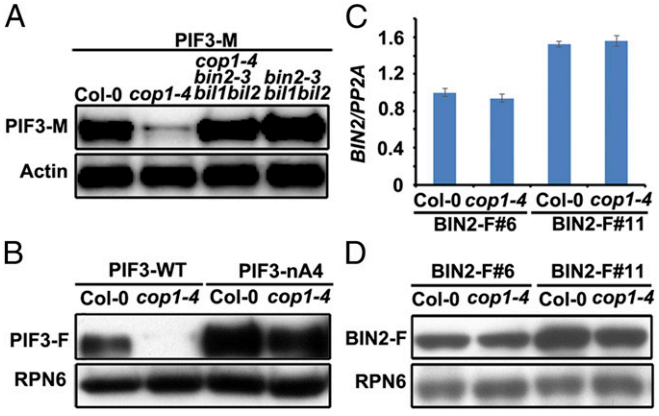

Fig. 4. COP1/SPA inhibits BIN2-mediated PIF3 destabilization. (*A*) Levels of PIF3-M in Col-0, *cop1-4*, *cop1–4 bin2-3 bil1 bil2*, and *bin2-3 bil1 bil2*. Actin was used as a loading control. (*B*) Protein gel blot of PIF3-WT-Flag and PIF3-nA4-Flag (PIF3-nA4) in Col-0 and *cop1–4*, respectively. RPN6 was used as a loading control. PIF3-F, PIF3-Flag. (*C*) mRNA levels of *BIN2-Flag* (*BIN2-F*) in Col-0 and *cop1–4*. Data shown are representative of two independent lines. (*D*) Protein levels of BIN2-F in Col-0 and *cop1–4*. RPN6 was used as a loading control.

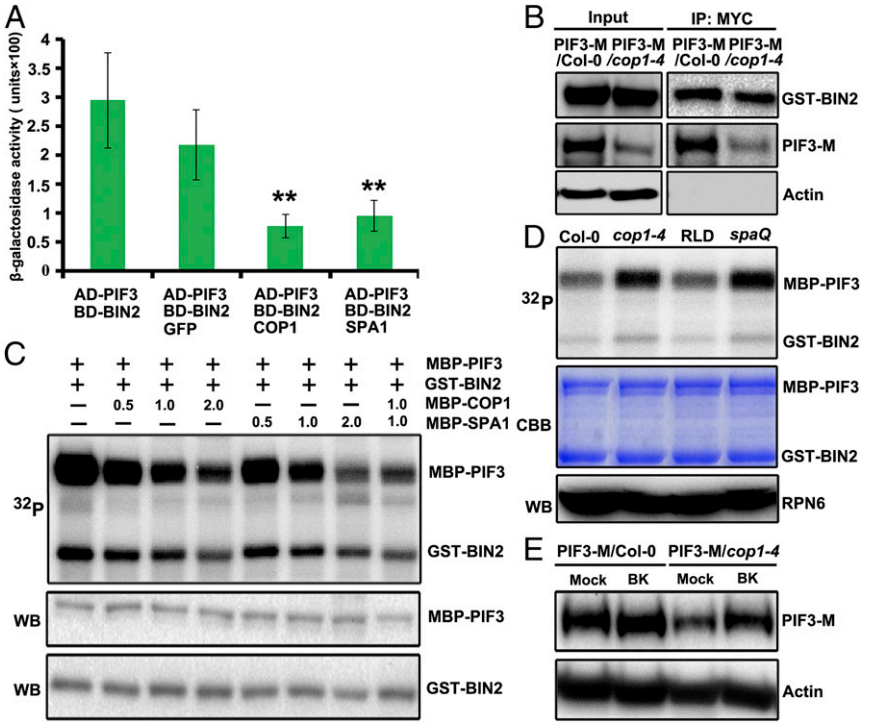

Fig. 5. COP1/SPA complex inhibits BIN2-mediated phosphorylation and degradation of PIF3. (*A*) Yeast three-hybrid assays showing the COP1 and SPA1 inhibition of the BIN2–PIF3 interaction in yeast cells. Data are Mean ± SD, $n = 3$. $^{**}P < 0.01$ (*t* test). (*B*) The Co-IP assays showing a stronger interaction between GST-BIN2 and PIF3 in the absence of COP1. Actin was used as a loading control. (*C*) COP1/SPA1 inhibits BIN2-mediated phosphorylation of *PIF3* in vitro. The quantity (micrograms) of MBP-COP1 or MBP-SPA1 added in the reaction mix was as indicated. (*D*) Cell-free kinase assays showing the phosphorylation levels of the MBP-PIF3 in the total extracts of dark-grown Col-0, *cop1–4*, RLD, and *spaQ* seedlings. (*Top*) the autoradiogram of MBP-PIF3; (*Middle*) CBB staining of the gel; (*Bottom*) RPN6 was used as a loading control. (*E*) Protein gel blot of PIF3-M in Col-0 and *cop1–4* treated with or without 30 μM BK. Actin was used as a loading control.

suggesting that the interaction of PIF3 with BIN2 is stronger in the absence of COP1/SPA complex (Fig. 5*B*).

COP1/SPA Complex Suppresses BIN2-Mediated PIF3 Phosphorylation and Degradation. To substantiate whether the interference of BIN2–PIF3 interaction by COP1/SPA1 complex would reduce BIN2 kinase activity toward PIF3, we first carried out in vitro kinase assays. When an increased amount of MBP-COP1 or MBP-SPA1 was added in the kinase reaction mix, phosphorylation levels of PIF3 were gradually decreased (Fig. 5*C* and Fig. S6), supporting the inhibitory effect of COP1 and SPA1 on PIF3 phosphorylation by BIN2. Interestingly, when MBP-COP1 and MBP-SPA1 were assayed together in the molecular molar ratio 1:1, a decrease of the phosphorylation level of PIF3 was further enhanced, compared with that of PIF3 with the addition of the same amount of COP1 or SPA1 alone. This finding suggested the role of COP1 working in concert with SPA1 in repressing the phosphorylation of PIF3 by BIN2.

To determine this inhibitory effect in plant cells, we designed a cell-free kinase assay by incubation of total extracts derived from the seedlings of Col-0, *cop1–4*, RLD (Rschew–Starize), and *spaQ*, each supplemented with equal amount of MBP-PIF3 and GST-BIN2. Phosphorylation levels of PIF3 were obviously higher in *cop1–4* and *spaQ* than WT (Fig. 5*D*), strongly suggesting that the phosphorylation of PIF3 by BIN2 is inhibited by the COP1/SPA complex in the dark. In agreement with this result, the specific GSK3-like kinase inhibitor bikinin (BK) (30) treatment of the transgenic seedlings overexpressing PIF3-M resulted in significantly higher accumulation of PIF3-M in the *cop1–4* mutant, but not in WT (Fig. 5*E*). Taken together, these data suggest that the instability of PIF3 in the mutants of COP1/SPA complex in darkness appears to have resulted from the increased phosphorylation levels of PIF3 by BIN2.

Discussion

Recent advances have suggested that the COP/DET/FUS group proteins and PIFs act coordinately to repress photomorphogenesis phenotypically and biochemically (15). However, the relationship between factors in those two groups requires further investigation. In this study, our findings provide an insight on the positive regulation of COP1/SPA complex on PIF3 stability bridged by the GSK3-like protein kinase BIN2, which unveils a noncanonical function of COP1/SPA complex in repressing photomorphogenesis in the model plant *Arabidopsis*.

To date, several lines of evidence have addressed the functional interaction of COP1 and SPA proteins with PIFs in different schemes of light-mediated plant growth and development. For example, $CUL4^{COP1–SPA}$ E3 ligase mediates the degradation of PIF1 upon light illumination (25). Alternatively, PIFs were reported to function as cofactors of the COP1/SPA1 E3 ligase complex to enhance its activity (31, 32). Moreover, to regulate photomorphogenic development, COP1 promotes PIF3-LIKE1 degradation to relieve its inhibition on transcriptional activity of PIFs (33). In addition, under shade conditions, COP1 enhances the activity of PIF family transcription factors by degrading HFR1 (34). Together, all these data pinpoint the function of COP1/SPA as being an E3 ligase in regulating or regulated by PIFs. Interestingly, in this work we discovered that in darkness COP1/SPA complex promotes the stability of PIF3, most likely through a nonproteolytic regulation on BIN2, the kinase of PIF3. From our data, we assumed that COP1 and the representative SPA protein SPA1 may have different role in repressing the BIN2–PIF3 interaction, in which COP1 functions possibly through sequestration of BIN2, whereas SPA1 works via the competitive interaction of the same regions of PIF3 with BIN2.

It's been reported that light-induced PIF3 phosphorylation is a prerequisite for its ubiquitination and degradation in the light (22). Our data suggest that the phosphorylation of PIF3 mediated by BIN2 also drives its proteasomal degradation in the dark. Moreover, the use of different cassettes of phosphorylation sites and likely distinct kinase systems are evident in the PIF3 degradation regulation in the dark or upon light illumination. Therefore, further characterization and comparison of the different kinase systems for PIF3 in darkness and under light conditions will be of particular relevance.

BIN2, the representative GSK3-like kinase in plants, has been found to be involved in many developmental processes, including skotomorphogenesis (35). A previous study and this work indicated that through the typical phosphorylation motifs on distinct sequences, BIN2 phosphorylates PIF3 and PIF4, respectively (27). Because PIF proteins accumulate in the dark, the regulatory mechanism for controlling BIN2 activity requires better exploration. The dephosphorylation or deacetylation of BIN2 has been shown to inhibit its activity in BR signaling (36, 37). Additionally, the relocalization of BIN2 to the plasma membrane restricts its activity during phloem differentiation (38). In skotomorphogenesis, our evidence pinpoints a key role of COP1/SPA complex in repressing BIN2 kinase activity. In mammalian cells, GSK3β, the orthologous of *Arabidopsis* BIN2, was reported to cooperate with MmCOP1 to inhibit breast tumor progression and metastasis by promoting the degradation of transcription factor c-Jun (39). Further elucidating of the precise mechanism by which the COP1/SPA complex regulates GSK3-like kinases, as represented by BIN2, will provide insights linking the functional interactions between the two types of key regulators in eukaryotes.

Materials and Methods

Plant Materials and Growth Conditions. The ecotypes of all WT *Arabidopsis thaliana* used in this study were Col-0 and RLD. The *cop1–4*, *spaQ*, and *pif3-3* mutants were reported previously (10, 40). Seed sterilization, stratification, and standard seedling growth experiments were performed according to the methods previously outlined (10). Four-day-old dark-grown seedlings were used in this study unless otherwise stated. For MG132 treatment, seedlings were grown in the dark for 4 d without or with 100 μM MG132 pretreatment for 6 h before harvesting.

Plasmid Construction and Generation of Transgenic Lines. To generate activation domain (AD)-PIF3 constructs for yeast two-hybrid assays, fragments containing full-length PIF3 coding sequence (CDS) (1–524 aa), and truncated PIF3 CDS including D1 (1–180 aa), D2 (181–524 aa), D3 (181–338 aa), and D4 (339–524 aa) were amplified and inserted into the EcoRI/XhoI sites of the pB42AD vector (Clontech). For AD-COP1 and AD-SPA1 constructs, fragments encoding full-length SPA1 and COP1, COP1N (1–127 aa) and COP1C (128–675 aa) were each amplified and inserted into the EcoRI/XhoI sites of the pB42AD vector. For DNA-binding domain (BD)-COP1 and BD-BIN2 constructs, DNA fragments encoding full-length COP1 and BIN2 CDS were amplified and inserted into the EcoRI/BamHI sites of the pLexA vector (Clontech). For BD-SPA1 constructs, DNA fragments encoding full-length SPA1 CDS (1–1,029 aa), SPA1N (1–545 aa), and SPA1C (546–1,029 aa) were amplified and inserted into the NcoI/XhoI sites of the pLexA vector. For yeast three-hybrid, DNA fragments encoding SPA1 and GFP were amplified and inserted into KpnI/XhoI sites of pGAD-T7 vector (Clontech).

For purification of MBP-PIF3 and GST-BIN2 recombinant proteins, BamHI /SalI DNA fragments encoding full-length or mutated PIF3 were cloned into the pMAL-c2x vector (New England Biolabs); an EcoRI/SalI DNA fragment encoding full-length BIN2 coding sequence was cloned into pGEX-4T-1 vector (GE Healthcare).

To generate nLUC-PIF3, a KpnI/SalI DNA fragment encoding full-length PIF3 coding sequence was cloned into pCAMBIA-nLuc vector. For cLUC-SPA1 and cLUC-BIN2 constructs, a KpnI/SalI and KpnI/BamHI DNA fragment encoding full-length SPA1 and BIN2 coding sequences, respectively, were each cloned into pCAMBIA-cLuc vector.

To generate Flag-tagged BIN2 and PIF3 transgene, DNA fragments containing full-length BIN2 and PIF3 coding sequences were each amplified and inserted into BamHI/SalI sites of pCAMBIA1307-3xFlag. For stable transformation, *Agrobacterium tumefaciens* bacteria strain GV3101 carrying those constructs were then transformed into Col-0 using the floral-dip method (41). At least two independent transgenic lines were selected. All of the cloning primers are listed in Table S1.

Western Blot and Antibodies. Protein extraction and immunoblots were performed as previously described (29). Antibodies used in this study were anti-COP1 (10), anti-PIF3 (29), anti-RPN6 (42), anti-RPT5 (42), anti-Actin (Sigma), anti-Flag (Sigma), anti-Tubulin (Sigma), anti-MYC (Sigma), anti-MBP (New England Biolabs), and anti-GST (New England Biolabs).

Cell-Free Degradation Assay. Cell-free degradation analyses were performed as previously described (43). In brief, 200 ng of MBP-PIF3 protein was incubated with individual extracts in the dark at 22 °C for the indicated time before collection. Anti-MBP and anti-RPT5 were used to analyze the results.

Yeast Two-Hybrid and Three-Hybrid Assays. Yeast two-hybrid assays were performed according to standard protocols (Clontech). Yeast three-hybrid assays were performed as described previously (44). β-Galactosidase activity was quantified with the yeast β-galactosidase assay kit (Thermo Scientific).

In Vitro Pull-Down and Co-IP. For in vitro pull-down assay, MBP fusion proteins (2 μg) and GST fusion proteins (1 μg) were incubated with 10 μL prewashed GST beads at 4 °C for 3 h. Eluted proteins were analyzed by immunoblotting using anti-MBP and anti-GST antibodies. For semi-in vivo Co-IP assay, 2 μg of recombinant proteins was mixed with 500 μg of total proteins extracted from the dark-grown seedlings in IP buffer (29), and subsequently incubated with 10 μL prewashed anti-MYC conjugated beads for 4 h at 4 °C. Eluted proteins were analyzed by immunoblotting using anti-MBP, anti-GST, and anti-MYC antibodies. For Co-IP assay, 500 μg of total proteins was incubated with 10 μL prewashed anti-Flag–conjugated beads for 3 h at 4 °C. Eluted proteins were analyzed by immunoblotting using anti-COP1 and anti-Flag antibodies.

LCI Assay. The LCI assay was performed as previously outlined with some modifications (45). In brief, *A. tumefaciens* bacteria strain GV3101 containing different constructs were injected in 4-wk-old *Nicotiana benthamiana* leaves. The plants were subsequently grown in darkness for 2 d before harvesting. The luciferase signals were analyzed with Night SHADE LB 985 (Berthold Technologies).

Quantitative RT-PCR. Total RNA was extracted from dark-grown seedlings by using the mini Plant RNA extraction Kit (Qiagen). One microgram of total RNA was reverse-transcribed using SuperScript II (Life Technologies) for synthesis of first strand cDNA. Quantitative RT-PCR (RT-qPCR) was performed using a 7500 Fast Real-Time PCR machine (Applied Biosystems). Primer sequences used for RT-qPCR are listed in Table S1. The gene-expression results were normalized by *PP2A*.

Kinase Assays. The in vitro and cell-free kinase assays were performed as previously described with some modifications (46). For in vitro kinase assay, MBP-PIF3 (1 μg) and GST-BIN2 (0.5 μg) were mixed into 20 μL of kinase buffer (20 mM Tris·HCl [pH 7.5], 100 mM NaCl, 12 mM $MgCl_2$, 0.1 mM ATP, 0.2 μCi [γ-^{32}P] ATP) with or without 20 μM BK. For the cell-free kinase assay, total proteins were extracted from Col-0, *cop1–4*, RLD, and *spaQ*, respectively, in the kinase buffer with 50 μM MG132 and 1 mM DTT. Five micrograms of total proteins were incubated with 1 μg MBP-PIF3 and 0.5 μg GST-BIN2. RPN6 was used as loading control. After incubation at 37 °C for 30 min, the samples were added into 1× SDS loading buffer and then boiled at 100 °C for 5 min to stop the reaction. Proteins were loaded and separated in 8% g/mL SDS/PAGE gel. Phosphorylation signals were detected using Typhoon FLA7000 (GE Healthcare).

ACKNOWLEDGMENTS. We thank Dr. Jianming Li for providing the *bin2-1* and *bin2-3 bil1 bil2* mutant seeds; Dr. Giltsu Choi for providing *35S:PIF3-HIS-MYC* line; and Dr. Yuqiu Wang, Dr. Fang Lin, Dr. Renbo Yu, and Kunlun Li for providing critical comments and the technical assistance. This work was supported by the National Natural Science Foundation of China Grants 31330048, 31621001, 91540105; National Basic Research Program (973 Program) Grant 2012CB910900; NIH Grant GM47850; and in part by the State Key Laboratory of Protein and Plant Gene Research at Peking University and the Peking-Tsinghua Center for Life Sciences.

1. Von Arnim A, Deng XW (1996) Light control of seedling development. *Annu Rev Plant Physiol Plant Mol Biol* 47:215–243.
2. Zhong S, et al. (2014) Ethylene-orchestrated circuitry coordinates a seedling's response to soil cover and etiolated growth. *Proc Natl Acad Sci USA* 111(11):3913–3920.
3. Lau OS, Deng XW (2012) The photomorphogenic repressors COP1 and DET1: 20 years later. *Trends Plant Sci* 17(10):584–593.
4. Leivar P, Quail PH (2011) PIFs: Pivotal components in a cellular signaling hub. *Trends Plant Sci* 16(1):19–28.
5. Zhong S, et al. (2009) EIN3/EIL1 cooperate with PIF1 to prevent photo-oxidation and to promote greening of *Arabidopsis* seedlings. *Proc Natl Acad Sci USA* 106(50): 21431–21436.
6. Shin J, et al. (2009) Phytochromes promote seedling light responses by inhibiting four negatively-acting phytochrome-interacting factors. *Proc Natl Acad Sci USA* 106(18): 7660–7665.
7. Deng XW, Caspar T, Quail PH (1991) *cop1*: A regulatory locus involved in light-controlled development and gene expression in *Arabidopsis*. *Genes Dev* 5(7):1172–1182.
8. Wei N, et al. (1998) The COP9 complex is conserved between plants and mammals and is related to the 26S proteasome regulatory complex. *Curr Biol* 8(16):919–922.
9. Yanagawa Y, et al. (2004) *Arabidopsis* COP10 forms a complex with DDB1 and DET1 in vivo and enhances the activity of ubiquitin conjugating enzymes. *Genes Dev* 18(17):2172–2181.
10. Zhu D, et al. (2008) Biochemical characterization of *Arabidopsis* complexes containing CONSTITUTIVELY PHOTOMORPHOGENIC1 and SUPPRESSOR OF PHYA proteins in light control of plant development. *Plant Cell* 20(9):2307–2323.
11. Leivar P, et al. (2009) Definition of early transcriptional circuitry involved in light-induced reversal of PIF-imposed repression of photomorphogenesis in young *Arabidopsis* seedlings. *Plant Cell* 21(11):3535–3553.
12. Leivar P, et al. (2008) Multiple phytochrome-interacting bHLH transcription factors repress premature seedling photomorphogenesis in darkness. *Curr Biol* 18(23): 1815–1823.
13. Shi H, et al. (2016) Seedlings transduce the depth and mechanical pressure of covering soil using COP1 and ethylene to regulate EBF1/EBF2 for soil emergence. *Curr Biol* 26(2):139–149.
14. Shi H, et al. (2016) The red light receptor phytochrome B directly enhances substrate-E3 ligase interactions to attenuate ethylene responses. *Dev Cell* 39(5):597–610.
15. Xu X, Paik I, Zhu L, Huq E (2015) Illuminating progress in phytochrome-mediated light signaling pathways. *Trends Plant Sci* 20(10):641–650.
16. Yi C, Deng XW (2005) COP1—From plant photomorphogenesis to mammalian tumorigenesis. *Trends Cell Biol* 15(11):618–625.
17. Holm M, Ma LG, Qu LJ, Deng XW (2002) Two interacting bZIP proteins are direct targets of COP1-mediated control of light-dependent gene expression in *Arabidopsis*. *Genes Dev* 16(10):1247–1259.
18. Seo HS, et al. (2003) LAF1 ubiquitination by COP1 controls photomorphogenesis and is stimulated by SPA1. *Nature* 423(6943):995–999.
19. Jang IC, Yang JY, Seo HS, Chua NH (2005) HFR1 is targeted by COP1 E3 ligase for post-translational proteolysis during phytochrome A signaling. *Genes Dev* 19(5):593–602.
20. Marine JC (2012) Spotlight on the role of COP1 in tumorigenesis. *Nat Rev Cancer* 12(7):455–464.
21. Nozue K, et al. (2007) Rhythmic growth explained by coincidence between internal and external cues. *Nature* 448(7151):358–361.
22. Al-Sady B, Ni W, Kircher S, Schäfer E, Quail PH (2006) Photoactivated phytochrome induces rapid PIF3 phosphorylation prior to proteasome-mediated degradation. *Mol Cell* 23(3):439–446.
23. Shen H, Moon J, Huq E (2005) PIF1 is regulated by light-mediated degradation through the ubiquitin-26S proteasome pathway to optimize photomorphogenesis of seedlings in *Arabidopsis*. *Plant J* 44(6):1023–1035.
24. Ni W, et al. (2014) A mutually assured destruction mechanism attenuates light signaling in *Arabidopsis*. *Science* 344(6188):1160–1164.
25. Zhu L, et al. (2015) CUL4 forms an E3 ligase with COP1 and SPA to promote light-induced degradation of PIF1. *Nat Commun* 6:7245.
26. Bu Q, et al. (2011) Phosphorylation by CK2 enhances the rapid light-induced degradation of phytochrome interacting factor 1 in *Arabidopsis*. *J Biol Chem* 286(14): 12066–12074.
27. Bernardo-García S, et al. (2014) BR-dependent phosphorylation modulates PIF4 transcriptional activity and shapes diurnal hypocotyl growth. *Genes Dev* 28(15):1681–1694.
28. Bauer D, et al. (2004) Constitutive photomorphogenesis 1 and multiple photoreceptors control degradation of phytochrome interacting factor 3, a transcription factor required for light signaling in *Arabidopsis*. *Plant Cell* 16(6):1433–1445.
29. Dong J, et al. (2014) *Arabidopsis* DE-ETIOLATED1 represses photomorphogenesis by positively regulating phytochrome-interacting factors in the dark. *Plant Cell* 26(9): 3630–3645.
30. De Rybel B, et al. (2009) Chemical inhibition of a subset of *Arabidopsis thaliana* GSK3-like kinases activates brassinosteroid signaling. *Chem Biol* 16(6):594–604.
31. Jang IC, Henriques R, Seo HS, Nagatani A, Chua NH (2010) *Arabidopsis* PHYTOCHROME INTERACTING FACTOR proteins promote phytochrome B polyubiquitination by COP1 E3 ligase in the nucleus. *Plant Cell* 22(7):2370–2383.
32. Xu X, et al. (2014) PHYTOCHROME INTERACTING FACTOR1 enhances the E3 ligase activity of CONSTITUTIVE PHOTOMORPHOGENIC1 to synergistically repress photomorphogenesis in *Arabidopsis*. *Plant Cell* 26(5):1992–2006.
33. Luo Q, et al. (2014) COP1 and phyB physically interact with PIL1 to regulate its stability and photomorphogenic development in *Arabidopsis*. *Plant Cell* 26(6):2441–2456.
34. Pacín M, Semmoloni M, Legris M, Finlayson SA, Casal JJ (2016) Convergence of CONSTITUTIVE PHOTOMORPHOGENESIS 1 and PHYTOCHROME INTERACTING FACTOR signalling during shade avoidance. *New Phytol* 211(3):967–979.
35. Youn JH, Kim TW (2015) Functional insights of plant GSK3-like kinases: Multi-taskers in diverse cellular signal transduction pathways. *Mol Plant* 8(4):552–565.
36. Hao Y, Wang H, Qiao S, Leng L, Wang X (2016) Histone deacetylase HDA6 enhances brassinosteroid signaling by inhibiting the BIN2 kinase. *Proc Natl Acad Sci USA* 113(37):10418–10423.
37. Kim TW, et al. (2009) Brassinosteroid signal transduction from cell-surface receptor kinases to nuclear transcription factors. *Nat Cell Biol* 11(10):1254–1260.
38. Anne P, et al. (2015) OCTOPUS negatively regulates BIN2 to control phloem differentiation in *Arabidopsis thaliana*. *Curr Biol* 25(19):2584–2590.
39. Shao J, et al. (2013) COP1 and GSK3β cooperate to promote c-Jun degradation and inhibit breast cancer cell tumorigenesis. *Neoplasia* 15(9):1075–1085.
40. Monte E, et al. (2004) The phytochrome-interacting transcription factor, PIF3, acts early, selectively, and positively in light-induced chloroplast development. *Proc Natl Acad Sci USA* 101(46):16091–16098.
41. Clough SJ, Bent AF (1998) Floral dip: A simplified method for *Agrobacterium*-mediated transformation of *Arabidopsis thaliana*. *Plant J* 16(6):735–743.
42. Kwok SF, Staub JM, Deng XW (1999) Characterization of two subunits of *Arabidopsis* 19S proteasome regulatory complex and its possible interaction with the COP9 complex. *J Mol Biol* 285(1):85–95.
43. Osterlund MT, Hardtke CS, Wei N, Deng XW (2000) Targeted destabilization of HY5 during light-regulated development of *Arabidopsis*. *Nature* 405(6785):462–466.
44. Huang X, et al. (2013) Conversion from CUL4-based COP1-SPA E3 apparatus to UVR8-COP1-SPA complexes underlies a distinct biochemical function of COP1 under UV-B. *Proc Natl Acad Sci USA* 110(41):16669–16674.
45. Chen H, et al. (2008) Firefly luciferase complementation imaging assay for protein-protein interactions in plants. *Plant Physiol* 146(2):368–376.
46. Cai Z, et al. (2014) GSK3-like kinases positively modulate abscisic acid signaling through phosphorylating subgroup III SnRK2s in *Arabidopsis*. *Proc Natl Acad Sci USA* 111(26):9651–9656.